SLAC – PUB – 3355
June 1984
(T)

Vacuum Structure of PQED in 2+1 Dimensions*

H. G. EVERTZ† AND D. HORN‡

Stanford Linear Accelerator Center
Stanford University, Stanford, California 94305

ABSTRACT

We present a numerical analysis of the vacuum structure of periodic QED in 2+1 dimensions. We use a Hartree-Fock ansatz of a bi-linear Gaussian wave-functional on which we impose the conditions of gauge-invariance and compactness. This ansatz has the correct structure in the weak-coupling limit and can be solved by employing a dilute-gas expansion. A numerical investigation substantiates the result of an exponentially increasing dynamical mass but deviates in detail from the analytic approximation. Using a Monte-Carlo program we obtain agreement with the dilute-gas approximation for weak-coupling, exhibit the behavior for strong-coupling and establish the viability of this form of analysis.

Submitted to *Physical Review D*

* This work was supported in part by the Department of Energy under Contract Number DE-AC03-76SF00515 and by the German Academic Exchange Service

† On leave from RWTH Aachen, W. Germany

‡ On leave from Tel-Aviv University, Israel

1. Introduction

The Hamiltonian of the $U(1)$ gauge theory (PQED) is

$$H = \frac{g^2}{2} \sum_{\ell} E_{\ell}^2 + \frac{1}{g^2} \sum_{p} (1 - \cos B_p) \tag{1.1}$$

where the electric field E_ℓ is defined on the link ℓ to be the canonical variable conjugate to the angle $0 \leq \theta_\ell \leq 2\pi$. B_p is the magnetic field defined on the plaquette p

$$E_\ell = -i \frac{\partial}{\partial \theta_\ell} \qquad B_p = (\nabla \times \theta_\ell)_p \ . \tag{1.2}$$

This is a confining theory in $2+1$ dimensions.[1]

Eliminating the gauge freedom

$$\theta_\ell \to \theta_\ell - (\nabla \alpha_i)_\ell \tag{1.3}$$

one realizes that the independent variables are the plaquette fields B_p. Describing the vacuum by a Hartree-Fock wave function, in which B_p plays the role of the conjugate momentum of a free field[2,3], one observes that the requirement that this ansatz be compact, i.e. invariant under the local transformation

$$\theta_\ell \to \theta_\ell + 2\pi N_\ell \tag{1.4}$$

leads to the appearance of a dynamical mass which signals confinement. This mass vanishes as $g \to 0$ with an essential singularity, which is also an expected feature of QCD in $3+1$ dimensions; hence the interest in investigating this problem.

Using a cluster expansion Suranyi[4] has obtained the following expression for the mass in this limit

$$m^2 = \frac{4\pi^2(\pi^2-4)}{g^4}\, e^{-\frac{\pi^2}{g^2 V}\sum_k D_k^{-1/2}} \tag{1.5}$$

where D_k denotes the negative of the lattice Laplacian in momentum space:

$$D_k = 4 - 2\cos k_1 - 2\cos k_2 \ . \tag{1.6}$$

This result has exactly the same characteristics as the solution by Göpfert and Mack [5] of the Euclidean version of this model in 3 dimensions.

We present a numerical investigation of the Hartree-Fock ansatz, a variational wave-function which incorporates the correct long-range correlations at weak-coupling and can interpolate throughout the whole range of g.[3] Our purpose is to calculate $m(g)$ for a finite range in g and establish the properties of this ansatz that can be obtained in a Monte-Carlo calculation.

In Chapter 2 we present a general formulation of our ansatz. The Hartree-Fock wave function is written for a non-compact link variable ϕ_ℓ. To relate it to θ_ℓ and impose compactness on the wave function we use an integer link field, and in order to render it gauge-invariant we use an auxiliary vertex field. In Chapter 3 we derive the weak-coupling expression for the energy by using a dilute-gas approximation for the curl of the integer link field. This expression is investigated numerically. We show that the minimum is obtained by a mass which is somewhat different from the analytic approximation (1.5) in the region $m \gtrsim 0.1$, where it becomes measurable. Chapter 4 describes our Monte-Carlo calculation. We find agreement with the dilute-gas approximation for weak-coupling and display data which exhibit the effect of compactness on confinement for strong-coupling.

2. The Hartree-Fock Ansatz

Let us start by setting up the ansatz in a form that does not presume the use of specific gauge-invariant variables. Our first task is to decompactify the angular variable. This is done by using

$$\Psi\Big(\{\theta_\ell\}\Big) = \int D\phi_\ell e^{-A(\{\phi_\ell\})} \prod_\ell \sum_{N_\ell} \delta\Big(\theta_\ell - \phi_\ell - 2\pi N_\ell\Big) \,. \tag{2.1}$$

ϕ_ℓ are non-compact link variables and N_ℓ are integers defined on links. To render our ansatz gauge-invariant we perform the projection[3]

$$P\Psi = \int D\alpha_i \; \Psi\Big(\{\theta_\ell - (\nabla\alpha_i)_\ell\}\Big) \tag{2.2}$$

with the $U(1)$ parameter α_i defined on the vertices of the lattice. This auxiliary field may be chosen to be non-compact. The norm of the resulting wave-function is

$$Z = \int D\theta_\ell \Psi^* P\Psi = \sum_{\{N_\ell\}} \int D\phi_\ell D\alpha_i e^{-A(\{\phi+\nabla\alpha+2\pi N\})} e^{-A(\{\phi\})} \tag{2.3}$$

and the expectation value of the Hamiltonian becomes

$$\langle H\rangle = Z^{-1} \sum_{\{N_\ell\}} \int D\phi_\ell D\alpha_i \, e^{-A(\{\phi+\nabla\alpha+2\pi N\})} H(\{\phi\}) \, e^{-A(\{\phi\})} \tag{2.4}$$

where the non-compact variable ϕ_ℓ replaces θ_ℓ in H.

We look now for an ansatz for $A(\{\phi\})$ which minimizes the ground state energy (2.4). We use a general bilinear Gaussian form

$$A(\{\phi_\ell\}) = \frac{1}{2} \sum_{\ell_1 \ell_2} \phi_{\ell_1} \Delta(\ell_1 \ell_2) \phi_{\ell_2} \tag{2.5}$$

where Δ has the Fourier decomposition

$$\Delta(\ell_1 \ell_2) = \frac{\delta_{\mu_1 \mu_2}}{V} \sum_k e^{i\vec{k}\cdot(\vec{j}_1 - \vec{j}_2)} c_{\vec{k}} \,. \tag{2.6}$$

In this expression the link ℓ is represented by its origin $\vec{j}$ and direction μ. The sum is carried out over all lattice momenta and V is the total volume (number of lattice vertices).

With this series of steps we have brought our problem into a form of statistical mechanics in 2 spatial dimensions. This allows the use of Monte-Carlo techniques for the evaluation of (2.4). For a given set of $c_{\vec{k}}$ one can easily generate ϕ fields in k-space whose distribution is determined by $e^{-A(\phi)}$. One may then randomly generate $\{\alpha_i\}$ and $\{N_\ell\}$ distributions to evaluate (2.4). Since the number of independent $c_{\vec{k}}$ is V it pays to start from some suitable parametrization that is motivated by a theoretical approximation. Such an expression is available in the $g \to 0$ limit.

3. The Dilute Gas Approximation

For the derivation of the weak-coupling limit it is useful to consider separately the longitudinal and transverse parts of the vector fields. In particular let us decompose the integer link variable into

$$N_\ell = \nabla \eta_i + \nabla \times \epsilon_p \tag{3.1}$$

where η_i and ϵ_p are vertex and plaquette fields respectively obeying Laplace equations with integer sources

$$\nabla^2 \eta_i = \nabla \cdot N_\ell \qquad \nabla^2 \epsilon_p = -\nabla \times N_\ell \; . \tag{3.2}$$

In our 2-dimensional problem ϵ_p is understood to point in the z-direction and the curl operator connects it to the N_ℓ field in the x- and y-directions. With this separation we may rewrite the exponential terms of (2.4) as

$$A(\phi + \nabla\alpha + 2\pi N) + A(\phi) = 2A(\phi') + 2A\Big(\frac{\nabla\alpha'}{2}\Big) + 2A(\pi\nabla \times \epsilon) \tag{3.3}$$

where ϕ' and α' are the shifted fields

$$\phi' = \phi + \frac{\nabla\alpha'}{2} + \pi\nabla \times \epsilon \qquad \alpha' = \alpha + 2\pi\eta \; . \tag{3.4}$$

The electric term of the Hamiltonian depends on all variables whereas the magnetic term depends only on the transverse part. The longitudinal part of the integer field just shifts the α field and has no effect on the calculation. The integration over the fields ϕ and α can be carried out in closed form for the Gaussian distribution (2.6) but the transverse part of the integer field, $\nabla \times \epsilon$,

can be calculated only by approximation. Note however that its distribution can be simply expressed as

$$2A(\pi\nabla\times\epsilon) = -\pi^2\sum_k \rho(k)\,\rho(-k)\,\frac{c_k}{D_k} \tag{3.5}$$

where $\rho(k)$ is the Fourier transform of the source of the equation of motion of ϵ

$$\rho_p = -(\nabla\times N_\ell)_p\ .$$

The value of the energy can then be derived by using a cluster expansion whose underlying assumption is that the ρ field is a dilute gas of monopoles ($\rho = \pm 1$ at largely separated locations, $\rho = 0$ otherwise). In this limit one finds that

$$E_{DG} = \langle H\rangle = \frac{g^2}{2}\left[\frac{1}{2}\sum_k c_k - 2\pi^2\sum_k \frac{c_k^2}{D_k}e^{-M_2}\right] - \frac{V}{g^2}e^{-M_1}(1-4e^{-M_2}) + \frac{V}{g^2} \tag{3.6}$$

where

$$M_1 = \frac{1}{4V}\sum_k \frac{D_k}{c_k} \qquad M_2 = \frac{\pi^2}{V}\sum_k \frac{c_k}{D_k}\ .$$

The variation of the energy with respect to c_k can be solved analytically in the weak-coupling limit. It turns out that the ansatz

$$c_k = \frac{D_k}{g^2\beta\omega_k} \qquad \omega_k^2 = D_k + m^2 \tag{3.7}$$

minimizes (3.6) in the limit $g\to 0$ with β obeying the consistency condition

$$\beta^2 = e^{M_1}/(1-4e^{-M_2}) \to 1$$

and the mass given by

$$m^2 = \frac{4\pi^2(\pi^2-4-4\pi^2e^{-M_2})}{g^4}e^{-M_1-M_2}. \tag{3.8}$$

This ansatz may be interpreted as assigning to $\nabla \times \phi$ the role of a canonical momentum of a free field of mass m.

In the weak-coupling limit $M_1 \to 0$ and $M_2 \to \infty$. Eq. (3.8) can be approximated by using in the calculation of both M_1 and M_2 the values $\beta = 1$ and $m = 0$. Eq. (1.5) is a further simplification of this formula in which only the leading terms were kept. This approximation is presented as the dotted line in Fig. 1, where it is compared with the iterative solution of (3.8) (dashed line) and the result of minimizing E_{DG}. We have used the momentum space of a 9^2 lattice to construct the functions $M_{1,2}$ of (3.6) which are needed for the numerical evaluation of E_{DG} as well as m of (3.8) and (1.5). This lattice size was chosen in order to enable us to compare these results with the Monte-Carlo calculations which will be described in the next chapter.

The comparison between the different mass curves is carried out over a range of g in which the dilute gas approximation holds. We find that the mass obtained by the numerical minimization lies lower than the analytic approximation but has the same exponential trend. The value of the mass is very sensitive to the value of β. Thus, for example, the mass values that are obtained by minimizing E_{DG} for $\beta = 1$ lie outside the scale of Fig. 1. Over the range $0.65 < g < 0.8$ we find that the best β (for which E_{DG} has a global minimum and m obtains the displayed values) increases linearly between $1.12 \lesssim \beta \lesssim 1.19$.

A very important feature of the numerical evaluation is that the variation of β and m leads to only minute changes in the energy, hence the minimum of E_{DG} in the (β, m) plane is very shallow. Characteristic values of $\frac{1}{E}\frac{\partial E}{\partial m}$ are of order 10^{-8}. This is so because the physical effect that we are looking at is tunneling between vacua of different integer-field distributions. An example of an energy

surface is presented in Fig. 2. We show the case of $g = 0.8$ with β varying between 1.1 to 1.28. The minimum of the energy-density is obtained at $\beta = 1.19$ and $m = 0.542$ and its value is 0.874720. This shows us that it will be very difficult to find the optimal mass value by a Monte-Carlo calculation.

It is instructive to look for the solution to our problem with the integer-field turned off. This corresponds to using an ansatz which is gauge-invariant but is not compact. In this case one can solve for the energy within our Hartree-Fock wave-function in a closed form. The result can be read off (3.6) by dropping the e^{-M_2} terms:

$$E_{NC} = \frac{g^2}{4}\sum_k c_k - \frac{V}{g^2}e^{-\frac{1}{4V}\sum_k \frac{D_k}{c_k}} + \frac{V}{g^2} \tag{3.9}$$

In the weak-coupling limit this is solved by (3.7) with $m = 0$. This massless solution continues to be valid over a finite range of g with only β adjusting itself. The variation of the energy as well as β is displayed in Fig. 3. At $g = 1.13$ the strong-coupling solution takes over. This solution has energy-density $1/g^2$ and its wave-function is constant, i.e. it may be characterized as having $m = \infty$. We conclude that the non-compact approximation undergoes an abrupt transition from a massless mode to a completely confining one.

4. Monte-Carlo Calculations

It is to be expected from the analysis in the previous chapter that we will need highly accurate numerical results in order to establish the correct mass of the vacuum structure. The effect leading to the best mass is due to tunneling between different N values, and it is as small as a tunneling effect can be. We will first of all establish the region where the numerical results agree with the dilute-gas analysis and then move to stronger couplings.

We will quote results of calculations carried out for a 9^2 lattice. We found this lattice size to be a convenient compromise between our quest for accuracy and our wish to avoid exorbitant computer runs. The calculation proceeded in the following way. For a given set of values of β and m in our ansatz (3.7) we first generated the Gaussian distribution of ϕ' in k-space, anticipating the decomposition of the action according to (3.3). In a similar way we generated the distribution of $\nabla\alpha'$. Once this was done we used a Fourier transformation to generate the distribution of the same fields in configuration space. At this point we added the integer field using a Metropolis algorithm to satisfy also the last term of the action in (3.3). We worked directly with the plaquette field ρ_p. Had we imposed periodic boundary-conditions on the integer link fields, we would be restricted to monopole anti-monopole pairs. It is necessary to allow for free monopole distributions to reconstruct the correct results at weak couplings, especially so if one works on a small lattice. Once all the distributions were generated we reconstructed the original ϕ fields and measured the Hamiltonian. Typically we ran 500 iterations for each point (i.e. specified values of β, m and g).

For very weak couplings, $g \lesssim 0.6$, the integer-field is inactive and the energy

is well approximated by the non-compact expression E_{NC} of (3.9). Correspondingly, the Monte-Carlo calculations show that the mass vanishes. In order to make contact with the dilute-gas approximation, which should manifest itself above $g = 0.6$, we fix $\beta = 1$ and vary only m. An example of the resulting data for $g = 0.7$ is displayed in Fig. 4. Every data point shown here is based on 8000 iterations and took 8 minutes to compute on the 8 MIPS CPU of the IBM 3081. This is compared with the variation of E_{DG} ($\beta = 1$, $g = 0.7$). All data points agree very well with E_{DG} within the statistical errors.

The best m, which is obtained by varying also β, is much smaller: it is $m = 0.16540$ at $\beta = 1.143$. This is the value on the curve of Fig. 1 at $g = 0.7$. The analytic calculation of the previous chapter gives $E_{DG} = 0.898115$ at the minimum compared to $E_{DG} = 0.900596$ for $\beta = 1$ and $m = 0.84$, the one shown in Fig. 4. Since at this value of g we established that E_{DG} reproduces correctly the data, we can rely on the calculation of the "best m" value in the previous chapter and do not have to search for it numerically.

Varying g we find that the agreement with the dilute-gas approximation continues to hold throughout the range $g \lesssim 0.9$. After that we do not have a valid theoretical approximation to work with, nonetheless we can continue the Monte-Carlo investigation. Using a fixed value of β (e.g. 1) one finds that the mass increases with g for a while, and then reverses the trend and tends to zero. However massive solutions continue to exist for lower β values. A characteristic case, for $g = 1.5$, is shown in Fig. 5. It is particularly impressive to note the pronounced minimum observed here, in contrast to the shallow minimum for $g = 0.7$ displayed in Fig. 4. The $m \to \infty$ end of the curve, which represents the correct solution at $g \to \infty$ comes down and is much closer to the minimum value

of the curve, as expected.

An unpleasant surprise is found by varying β: we obtain vacua with all possible mass values, all of which have energy-densities of about 0.42 for $g = 1.5$. The two extrema are $m = 0$ for which $\beta = 1.4$ and the energy-density is 0.424 ± 0.001 , and $m \to \infty$ with $\beta = 0$ and $\beta m = 2.8$ for which the energy-density is 0.422 ± 0.002. The same value of βm is obtained for all $\beta \leq 0.5$. It is a tedious and costly procedure to find the lowest energy density. We found it to be around $m = 26$ and $\beta = 0.01$ for which we obtained an energy-density of 0.419 ± 0.001. All these values are close to the prediction 0.4226 of strong-coupling perturbation theory at $g = 1.5$.[6] Similar results were obtained when we limited ourselves to dipole ρ distributions. We conclude that the mass which governs the structure of the vacuum continues to grow with increasing coupling.

5. Summary

We have carried out a numerical analysis of a wave-functional that has been used until now for analytic approximations only. Our ansatz employs the correct behaviour of a free-field theory and is applicable in the weak-coupling domain of an asymptotically-free gauge-theory. This enables one to use a variational method directly in the weak- coupling regime, which is the interesting region for QCD. In this paper we have demonstrated the viability of this approach on a simpler problem which has similar characteristics for weak-coupling.

As the first step we decompactify our link-variable and introduce auxiliary fields which guarantee gauge-invariance and compactness. The Hartree-Fock wave-functional of the new non-compact variable depends on a mass-parameter which sets the scale of all correlations. This is a dynamically generated mass

which vanishes in the weak-coupling domain with an essential singularity. This non-perturbative behaviour is due to the compactness of the theory (and of the vacuum), and can therefore be traced back to the integer field that we use to guarantee compactness. Using a cluster-expansion we solve this problem analytically and numerically for weak couplings. The analytic solution involves further assumptions and turns out to be different from the numerical answer in the region where the mass becomes measurable.

After establishing the correct behaviour of the dilute-gas approximation, we turn to a Monte-Carlo analysis and check it in the weak-coupling domain. The results are very encouraging. We are able to obtain the correct behaviour over the entire domain in which we can check it, and we can extend the method into the strong-coupling region as well. We find, as expected, that the dynamically-generated mass increases strongly with the coupling.

This method requires large amounts of computer time because it involves an iteration scheme which is non-local on the lattice. This is an obstacle in the way of its application to interesting non-abelian problems. Hopefully one can develop further refinements and shortcuts that will enable one to apply a similar analysis to QCD in the foreseeable future.

ACKNOWLEDGMENT

We wish to thank M. Karliner for providing us with his computer program for generating a free-field vacuum.

REFERENCES

1. A. M. Polyakov, Phys. Lett. 59B (1975) 82; Nucl. Phys. B120 (1977) 429. T. Banks R. Myerson and J. Kogut, Nucl. Phys. B129 (1977) 493. J. Villain, J. Phys. 36 (1975) 581. M. Peskin, Ann. Phys. (N.Y.) 113 (1978) 122.
2. S. D. Drell, H. R. Quinn, B. Svetitsky and M. Weinstein, Phys. Rev. D19 (1979) 619.
3. D. Horn and M. Weinstein, Phys. Rev. D25 (1982) 3331.
4. P. Suranyi, Phys. Lett. 122B (1983) 279.
5. M. Göpfert and G. Mack, Comm. Math. Phys. 82 (1982) 545. J. Ambjorn, A. Hey and S. Otto, Nucl. Phys. B210 (1982) 347.
6. A. C. Irving, F. J. Owens and C. J. Hamer, Phys. Rev. D 28 (1983) 2059.

FIGURE CAPTIONS

1. Mass curves for the dilute-gas approximation. The full line represents the result of numerical minimization of E_{DG}. The dashed curve is the iterative solution of the analytic approximation (3.8) and the dotted curve is the result of (1.5).
2. The energy-density in the dilute-gas approximation at $g = 0.8$ is displayed as a function of the mass for ten values of β varying from 1.1 to 1.28 by steps of 0.02.
3. The non-compact problem (3.9) displays an abrupt transition from a massless solution (whose energy is given by the full line and β by the dotted curve) to the strong coupling result (infinite mass) $E = 1/g^2$.
4. Results of the Monte-Carlo calculation show complete agreement with the dilute-gas approximation (full curve) for $g = 0.7$ and $\beta = 1$.
5. Monte-Carlo analysis at $g = 1.5$ displays a clear minimum at $m = 1.7$ for $\beta = 1$.

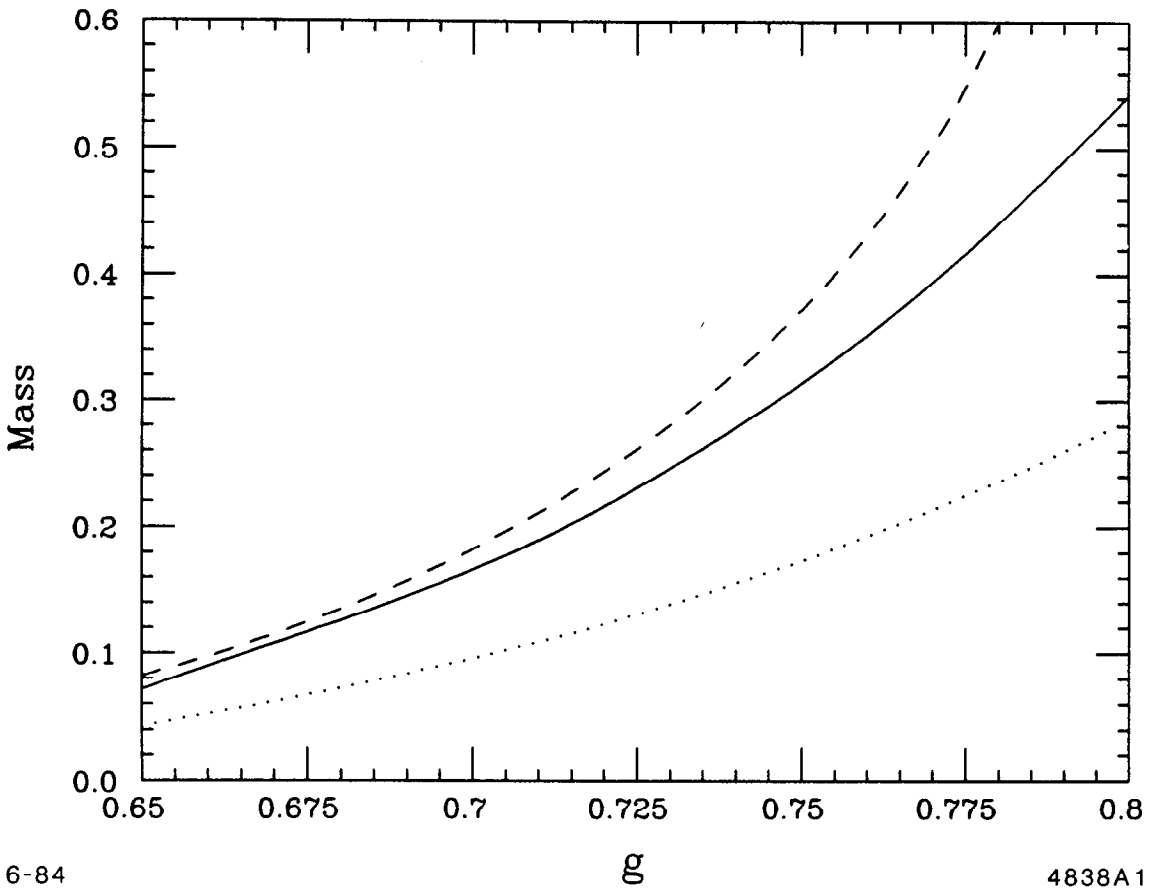
0.6
0.5
0.4
0.3
0.2
0.1
0.0
Mass
0.65
0.675
0.7
0.725
0.75
0.775
0.8
g
6-84
4838A1

Fig. 1

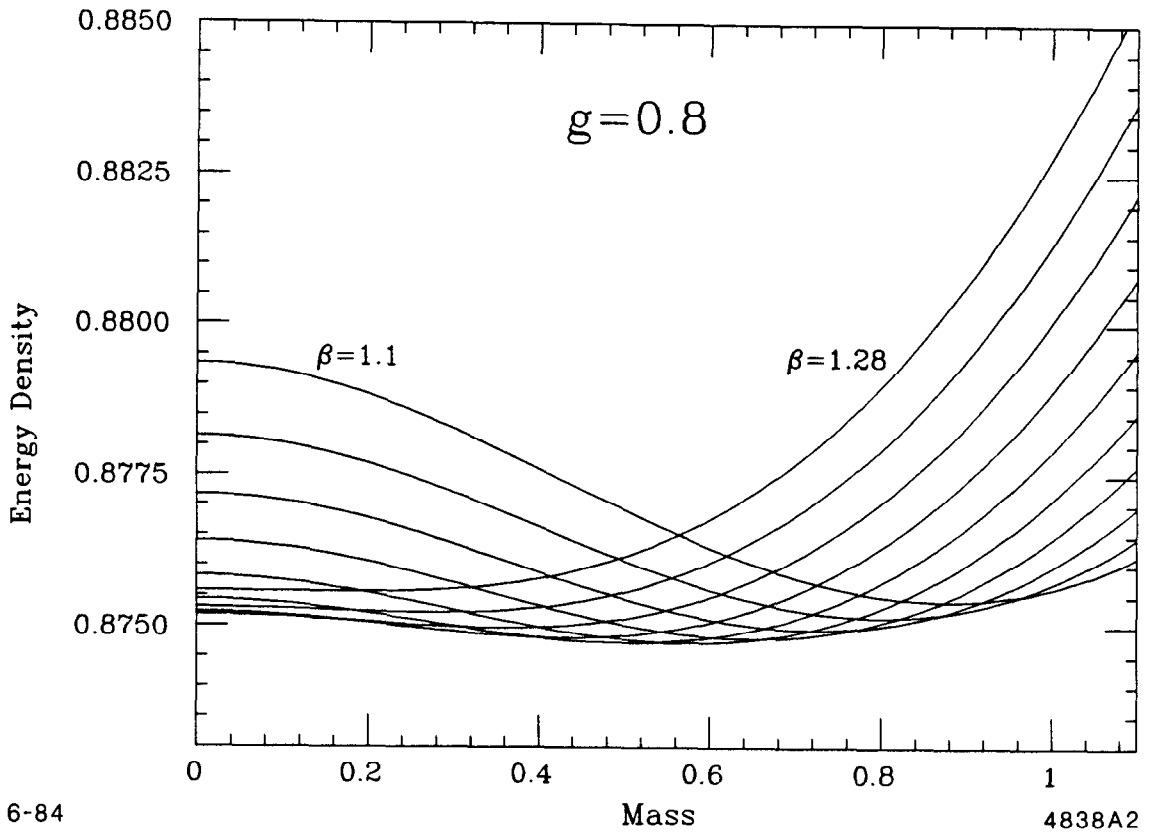
g=0.8
β=1.1
β=1.28
Energy Density
0.8850
0.8825
0.8800
0.8775
0.8750
0
0.2
0.4
0.6
0.8
1
Mass
6-84
4838A2

Fig. 2

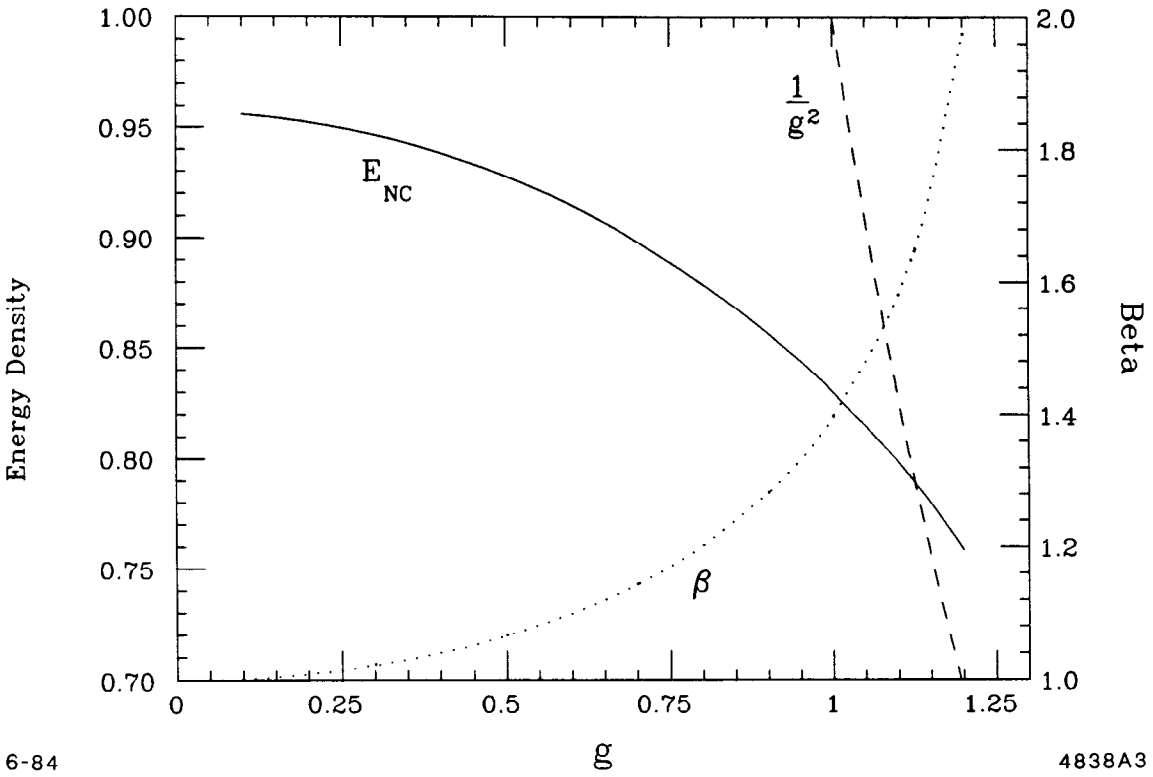
1.00
0.95
0.90
0.85
0.80
0.75
0.70
Energy Density
2.0
1.8
1.6
1.4
1.2
1.0
Beta
0
0.25
0.5
0.75
1
1.25
g
E_{NC}
$\frac{1}{g^2}$
β
6-84
4838A3

Fig. 3

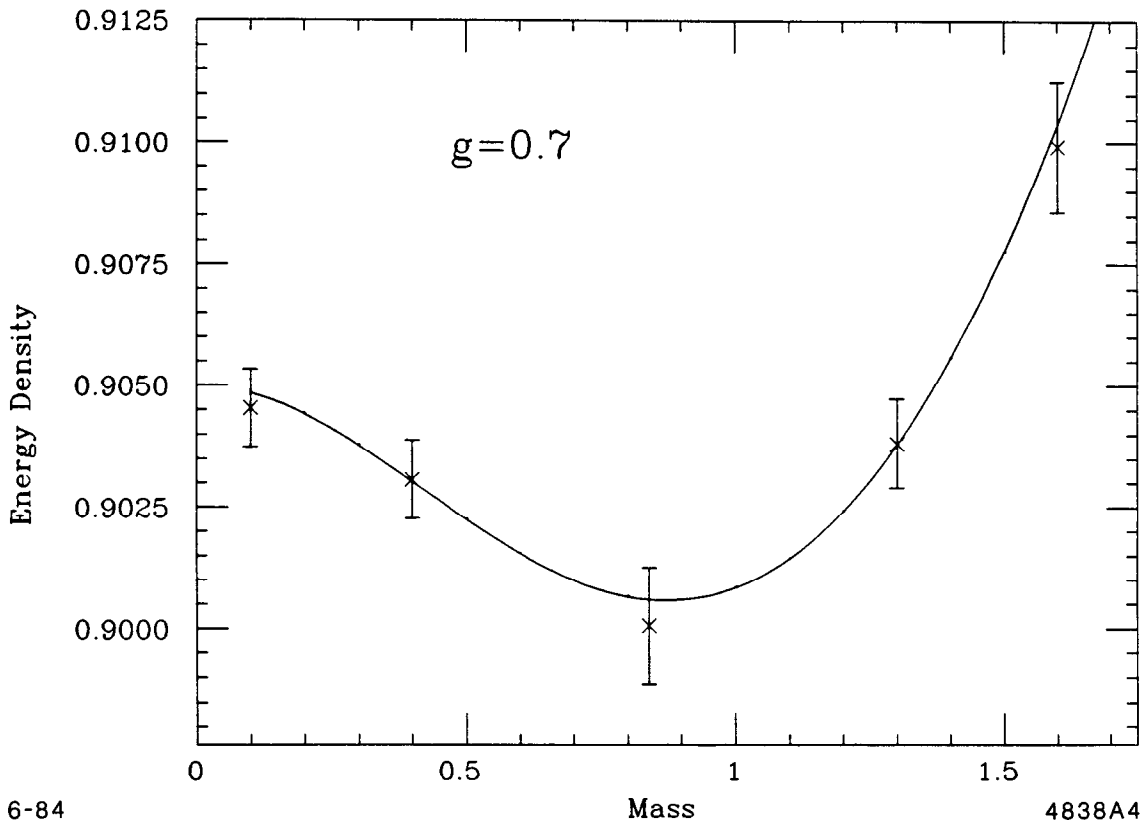
0.9125
0.9100
0.9075
0.9050
0.9025
0.9000
g=0.7
Energy Density
0
0.5
1
1.5
Mass
6-84
4838A4

Fig. 4

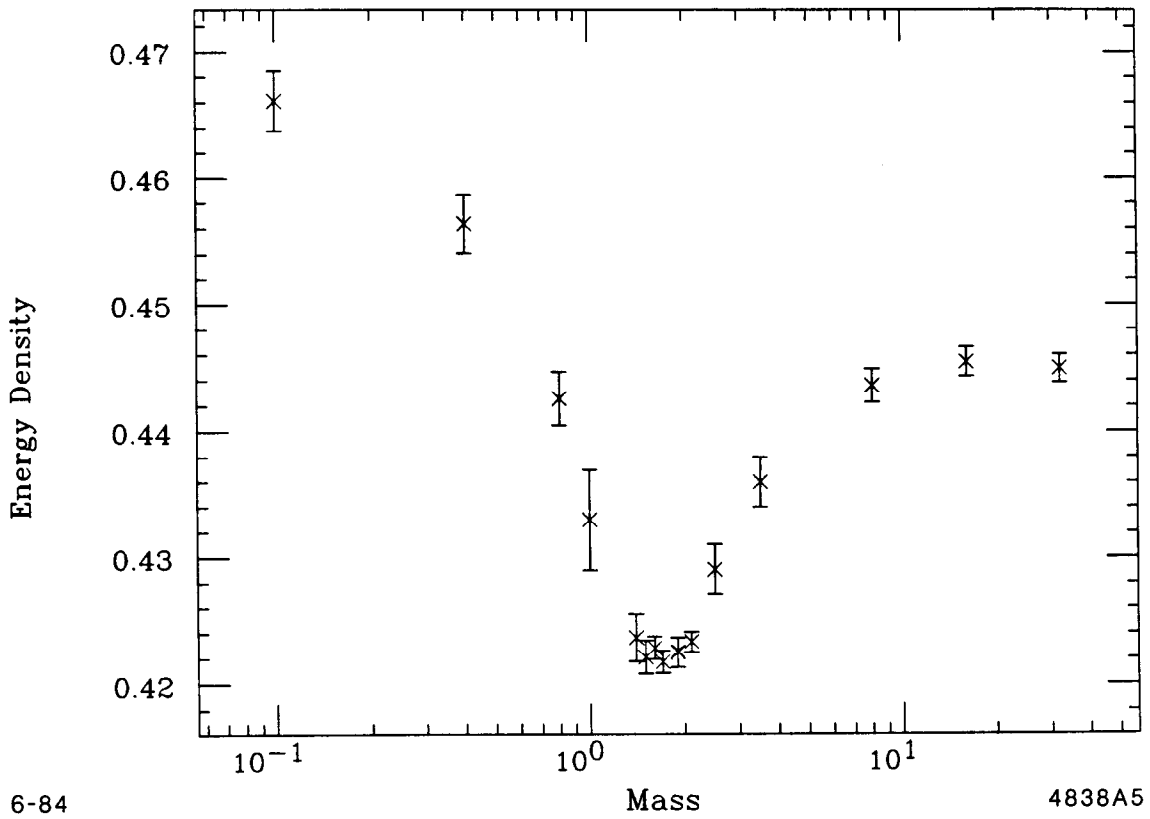
0.47
0.46
0.45
0.44
0.43
0.42
Energy Density
10^{-1}
10^{0}
10^{1}
Mass
6-84
4838A5

Fig. 5